

---

30-31 October 2024

# Assessment of zirconia thermal barrier coatings on austenitic steel

---

Savin A.<sup>\*1</sup>, Steigmann R.<sup>1</sup>, Faktorova D.<sup>2</sup>

1. Nondestructive testing Department, National Institute of R&D for Technical Physics, Iasi, Romania; steigmann@phys-iasi.ro
  2. Faculty of Special Technology, Alexander Dubcek University of Trenčín, Trenčín, Slovakia; dagmar.faktorova@tnuni.sk
- \*Corresponding author: asavin@phys-iasi.ro

**Abstract:** *The need to increase the efficiency of aerodynamic engines and last generation turbines ( $t > 1200^\circ\text{C}$ ) have imposed new types of materials and coating techniques for the realization of thermal barriers (TBCs). Yttria-doped zirconia (YSZ)-based TBCs are now competing with new materials to provide durability and reliability. The research is focused on the development of new TBC manufacturing techniques to improve the performance of YSZ. A layer of zirconia, without intermediate thermally grown oxide (TGO), with micrometric thickness of the deposition on an austenitic steel support, multilayered and doped with nanometric particles in two phases, was investigated non-destructively. The results obtained on the quality and adhesion to the support obtained by X ray diffraction (XRD) and scanning electron microscopy (SEM) are compared with the electromagnetic ones (EM).*

**Keywords:** *ZrO<sub>2</sub>-ceramic coating, yttria, SEM, XRD, nondestructive testing*

## 1. INTRODUCTION

In the evolution of industrial sectors involving gas turbines, the innovative advances related to ceramic protective coatings at high temperatures, Thermal Barrier Coatings (TBCs) are of particular importance. The literature includes a large number of specialized works that provide information on some aspects of the behavior of TBCs [1-3] at high temperatures. Among them, we also find those focused on the comprehensive analysis of the mechanisms underlying spalling ceramic zirconia ceramic as TBCs, in terms of material selection, deposition techniques, performance evaluation, etc. TBCs are the most difficult and delicate structures that must ensure the protection of engines from the unwanted effects of extreme operating temperatures in power generating units[4]. New generations of materials based on rare earths have been developed in the manufacture of TBCs aiming to increase efficiency, improve durability and reduce the cost of the life cycle [5],[6]. Ceramic coating (CC) part of TBC creates a protective layer and together with the base material forms a layered composite of refractory oxide with a small thickness (approx. 120-400 $\mu\text{m}$ ). The typical CC architecture has two layers, a top coating layer that ensures thermal insulation, usually a ceramic with a low thermal conductivity, and an antioxidized layer that ensures adhesion to the superalloy

substrate (bond coat BC). TBC can be obtained through the atmospheric plasma spraying (APS) process [7] or electron beam physical vapor deposition (EB-PVD) technology in bi- or multi-layered structures and represent favorable models for coatings [4]. Whatever the advantages/disadvantages of high-performance TBC deposition methods, they must ensure superior resistance to thermal shocks, erosion and excellent thermal efficiency. Besides these, the implementation of TBC has the advantage of reducing the possibility of using a variety of fuels (especially for stationary gas turbines). Zirconia ( $ZrO_2$ ) stabilized with yttria (YSZ) is most often used as a material for thermal coatings in engines due to its high resistance to thermal shocks, high oxidation and thermal fatigue resistance up to  $1150^\circ C$ . The objective of the work is to emphasize, by combining non-destructive evaluation (NDT) techniques (electromagnetic EM, X-ray diffraction and SEM with Dispersive X-ray spectroscopy), the effect of doping with nano particles  $Y_2O_3$  of the YSZ ceramic structure used as TBC.

## 2. MATERIALS AND METHODS

The most vulnerable part of a thermal barrier (TB) is the ceramic substrate interface. Cracking due to high temperatures and intergranular stress of 316L and 304L stainless steel is a critical problem. In the present case, the AISI 316L austenitic steel alloy ( $<0.03\% C$  as EN 14404), susceptible to intergranular corrosion, is covered with YSZ ceramics considered TBC [8]. The laminar structures of YSZ as TBC are analyzed to emphasize the improvement of Zr coating-based ceramics properties as a function of addition of  $Re_2O_3$  in the structure of the original ceramics. Ceramics  $ZrO_2$  doped with rare earths (RE) oxides is considered a good TBC material due to their advanced mechanical properties such as low thermal conductivity ( $2.0\ m^{-1}K^{-1}$  at  $1100^\circ C$ ), refractory, corrosion resistance, as high-fracture toughness and bulk modulus, chemical inertness, and compatible thermal expansion coefficient] with metallic support [9]. At the nanoscale, the main method of stabilizing the tetragonal phase (t) is the introduction of Ce or Y as stabilizing component. Pure yttrium oxide has high melting point; it is chemically inert and has an excellent electrical insulation. In a deposition like TBC, the most sensitive part is the substrate-ceramic interface, where  $t \rightarrow m$  transformations occur that can generate fractures under the influence of thermal shock. For YSZ ceramics, a superior layer quality can be obtained by glazing when the surface can be densified. CC were deposited onto AISI 316L samples [8], with  $80 \times 20 \times 2\ mm^3$  and were investigated through XRD, structure and SEM. The samples were sandblasted using 50-80 grit alumina to improve adhesion of the deposition to the substrate as well as to remove possible residues from the metal surface [10]. The formation and evolution of flaws (dislocations, cracks, voids, amorphous phases), as well as the interaction between grain boundaries (GB) and flaws are of interest to the  $ZrO_2$ . Among the intrinsic factors that govern the superplastic response of  $ZrO_2$  ceramics, chemical bonding state at GBs has been reported, the research being focused on the intergranular fracture surfaces of polycrystalline YSTZ [11]. Using YSZ ceramics, the quality of the CC applied to the metal surface of the substrate increases. Figure 1 shows the image of the  $ZrO_2$  coating on AISI surface, emphasizing the region formed by the CC before and after spraying with nano powder  $Y_2O_3$ . It can be considered that the densification obtained by spraying closes the voids that affect the

sandwich surface of the ceramic (figure 1b) which can lead to an increase in thermal conductivity [12]. These regions that create a densification can also be distinguished by microscopic visualization.

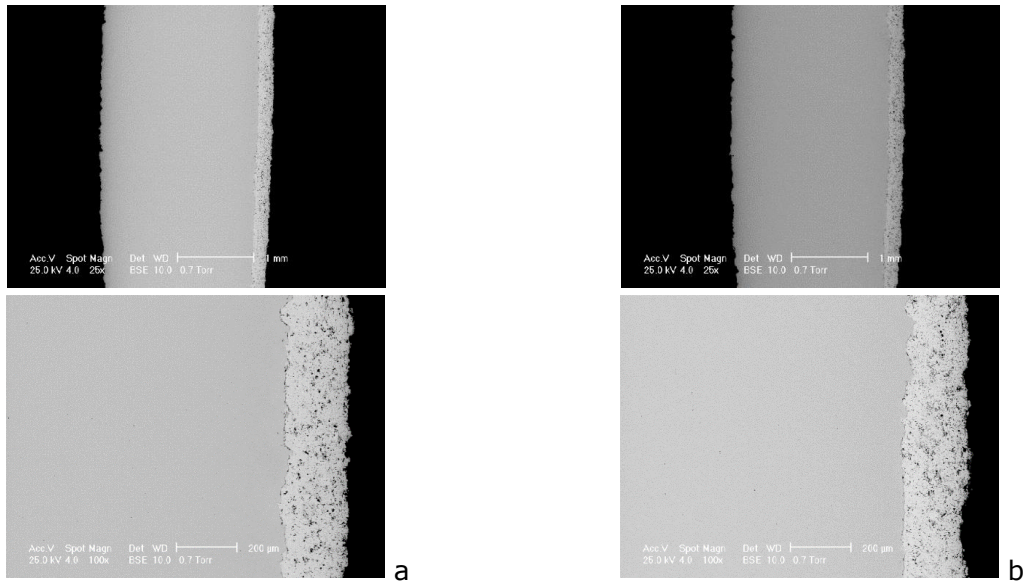


**Figure 1:** Support AISI 316L and sandwich of zirconia (a) for specimen with 0.2 mm thin monolithic coating  $ZrO_2$  with addition of 20 %  $Y_2O_3$ ; and (b) for specimen with sandwich coating 0.25 mm  $ZrO_2$  with addition of 20 %  $Y_2O_3$  and 0.005 mm  $Y_2O_3$ .

### 3. RESULTS AND DISCUSSIONS

#### 3.1. Microscopy and XRD analyses

The structures of YSZ layers appear porous (Figure 1a). The information about the action of sandwich coating nano powder 0.005mm  $Y_2O_3$  on the densification and adhesion to the support of CC on SS was obtained from Secondary Electrons (SE) images, as well as Backscattered Electrons (BSE) images (Figures 2 a;b).

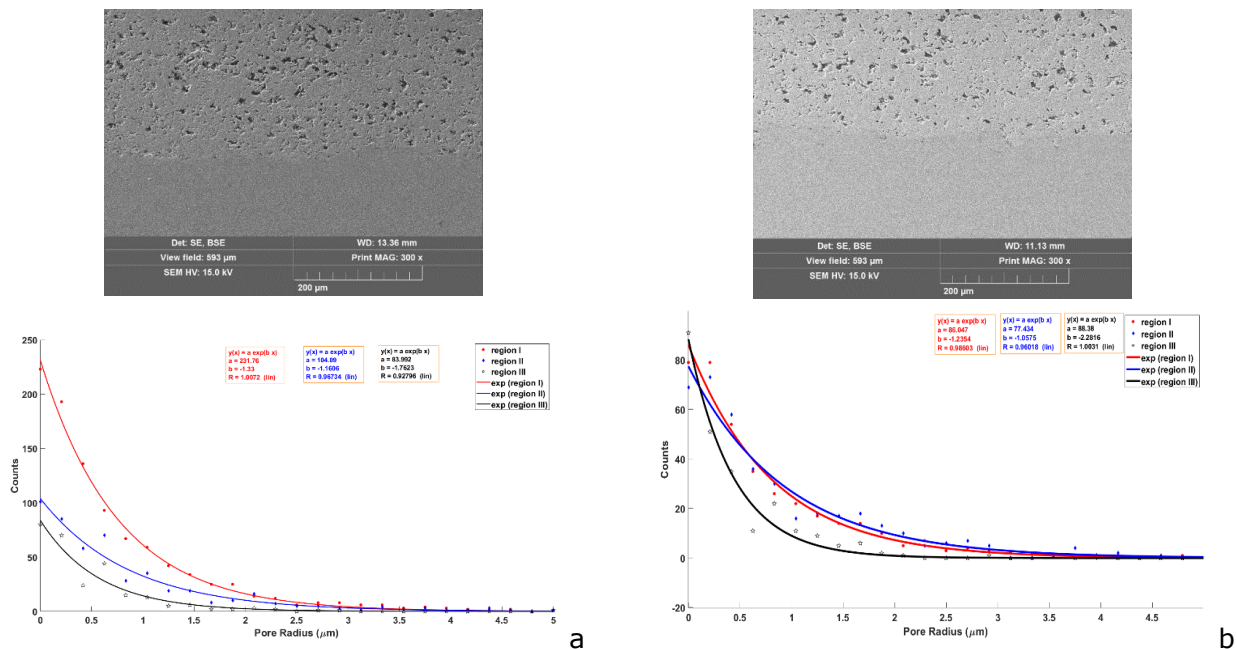


**Figure 2:** SEM images specimen with voids counting for (a) coating 0.25 mm thick monolithic coating  $ZrO_2$  with addition of 20 %  $Y_2O_3$  and (b) sandwich coating 0.25 mm  $ZrO_2$  with addition of 20 %  $Y_2O_3$  and 0.005 mm  $Y_2O_3$ .

In order to establish the pore distribution, the obtained image was divided equally to obtain three regions; region III includes the adhesion layer to the support. The doping with  $Y_2O_3$  caused a decrease in the number of large pores, and in the middle of the coating layer (region II), a densification can be observed. XRD experiments were performed at room temperature using a Philips diffractometer. The phase composition and microstructural parameters were determined using Fullprof software, Ceckcell was used for the spatial group and network constants.

The diffractogram for the sample containing the layer of  $ZrO_2$  doped with  $Y_2O_3$  on the SS support and the  $ZrO_2$  one doped with  $Y_2O_3$  were traced.

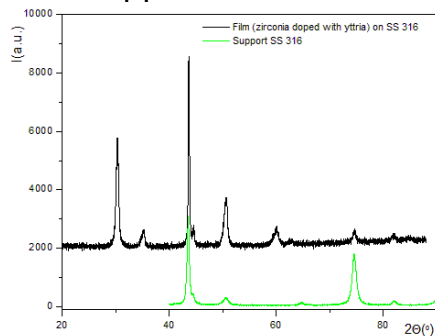


**Figure 3:** XRD of films and SS 316 support

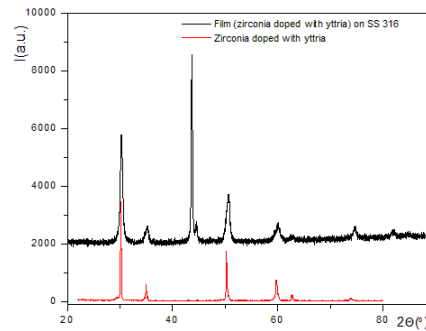


**Figure 4:** XRD of films and  $ZrO_2$  with yttria

These allowed the identification of the austenite maximum  $\gamma$  (Figure 3) and of the doping maxima t  $ZrO_2$  (Figure 4). The composition as shown in figures 5 and 6 were obtained using Energy Dispersive X-ray spectroscopy (EDXS).

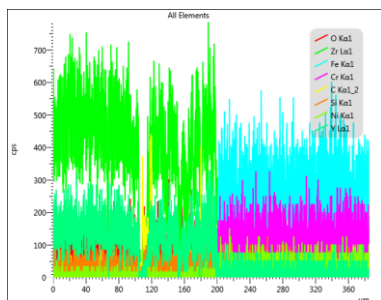


**Figure 5:** EDXS of  $(ZrO_2 + 20\% Y_2O_3)$  coating thick monolithic sandwich - 0.2mm)

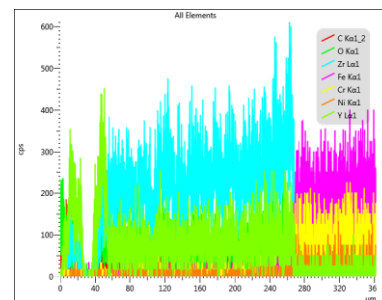


**Figure 6:** EDXS of  $(ZrO_2+20\%Y_2O_3)$  coating and 0.005 mm  $Y_2O_3$ )

### 3.2. Electromagnetic methods

NDT is based on the EM method, which is a method applied to conductive materials. The EM method consists in evaluating the interaction of the EM field and the material, the dependence of the transducer impedance on the material properties being known. Advantages such as high sensitivity automated scanning, non-contact inspection and detection of material discontinuities make this technique complementary to classical methods. The impedance changes due to the densification of ceramics or small variation of thickness are incoherent whereas the impedance changes due to defect extended spatially (adherence to the support) of eddy current of the transducer used are significantly. Experimental set-up is presented in figure 7. The working frequency of the transducer is 105MHz provided by Agilent 4395A, the data is acquired and stored on PC. Cracks may appear in the ceramic layer after deposition due to the relaxation of residual stresses.

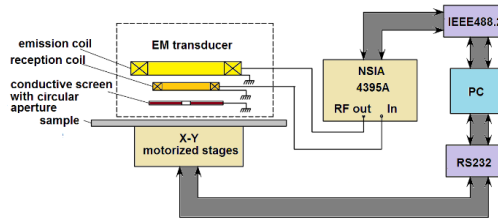


**Figure 7:** Experimental set-up

The microstructure can present lamellar washes or flattened with microcracks through washes or inter-washes. When scanning the surface of the sample, the image provided through the transducer is amplified. The EM field generated by the transducer propagates in the material as a wave with the wavelength  $\lambda=2\pi\delta$  where  $\delta = \sqrt{2 / \omega\mu_0\sigma}$ ,  $\omega=2\pi f$  angular frequency,  $\sigma$  electrical conductivity,  $\mu_0$  vacuum magnetic permeability. The detection principle is similar to that of near-field EM scanning microscopy [13].

In essence, it is about the technique of electron emission from the tip of the transducer and the interaction with the sample. As a result, the extracted electrons are ejected from the sample surface and detected by the transducer. The "topographic images" determined by the intensity variations of the secondary and backscattered electrons give a vertical resolution at the atomic scale and a small nanometric lateral one. The transducer works as a detection antenna transforming localized energy into electromotive forces.

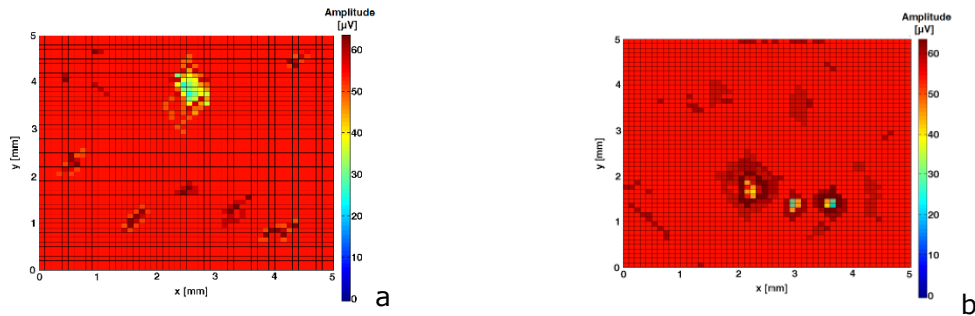


**Figure 8:** The amplitude of the emf induced in the reception coil of the EM transducer at the scanning of the specimens: a) 0.25 mm thick coating  $ZrO_2+20\% Y_2O_3$ ; b) sandwich coating 0.25 mm  $ZrO_2 + 20\% Y_2O_3$  and 0.005mm  $Y_2O_3$

The images show the amplitude of the emf induced in the reception coil of the EM transducer at the scanning of the surface of analyzed specimens. The image in Figure 8a corresponds to 0.25mm thick monolithic coating  $ZrO_2+20\% Y_2O_3$ , and shows, in addition to the lack of adhesion to the support, some inhomogeneities of the microstructure, possibly both in CC and on the surface of the support (SS AISI 316L). The image corresponding to the CC structure with 0.25mm  $ZrO_2+20\% Y_2O_3$  and 0.005mm  $Y_2O_3$ , shows that doping with yttrium nanopowder makes the voids more extensive while decreasing their number, an observation in agreement with the SEM results (Figure 2).

#### 4. CONCLUSIONS

The performance of CC based on zirconia doped with yttria can be increased by densifying the ceramic coating with yttria nanopowders. The multilayered

ceramic nanocomposite (realized as TBC) obtained by doping in two phases with yttria and structured in a gradient presents special characteristics compared to the ceramic coating realized as a thermal barrier through traditional YSZ. The reduction of the number of voids in the CC layer was highlighted as well as a good adhesion to the support, without thermally grown oxide (TGO) intermediate, of the CC layer with a micrometric thickness. The optimization of the TBC deposition methods and the evaluation of the CC performances, involves the analysis of the adhesion to the support and the increase of the life span. Additional tests are needed on a larger number of samples having CC with variable thicknesses and subjected to different thermal treatments to establish the accuracy of the results. It is necessary to establish a correlation between the decreasing number of voids and the concentration of yttria nanoparticles.

## Acknowledgements

This work was supported by MCID Nucleu (PN 23 11 01 02) and PFE (Contract No. 5PFE/2022) Programs.

## References

- [1] Wei Z.Y., et al. (2022). Progress in ceramic materials and structure design towards advanced thermal barrier coatings. *Journal of Advanced Ceramics*, 11(7), 985-1068
- [2] Mehta, A., et al. (2022). Processing and advances in the development of thermal barrier coatings: a review. *Coatings*, 12(9), 1318.
- [3] Thakare, JG, Pandey, C., Mahapatra, MM, & Mulik, RS (2021). Thermal barrier coatings—A state of the art review. *Metals and Materials International*, 27, 1947-1968.
- [4] Pakseresht, A., et al. (2022). Failure mechanisms and structure tailoring of YSZ and new candidates for thermal barrier coatings: A systematic review. *Materials & Design*, 222, 111044.
- [5] Meghwal, A., Anupam, A., Murty, BS, Berndt, CC, Kottada, RS, & Ang, ASM (2020). Thermal spray high-entropy alloy coatings: a review. *Journal of Thermal Spray Technology*, 29, 857-893.
- [6] Sudarshan, R., Venkatesh, S., & Balasubramanian, K. (2020). Thermal Barrier Coatings for Gas-Turbine Engine Applications-A Review. *PalArch's Journal of Archeology of Egypt/Egyptology*, 17(6), 15487-15500.
- [7] Vaßen, R., Mack, DE, Tandler, M., Sohn, YJ, Sebold, D., & Guillon, O. (2021). Unique performance of thermal barrier coatings made of yttria-stabilized zirconia at extreme temperatures (> 1500°C). *Journal of the American Ceramic Society*, 104(1), 463-471.
- [8] Savin, A., et al (2018). Complementary Methods for Evaluation of Yttria Stabilized Zirconia Coatings used as Thermal Barrier Coating. *Journal of Mechanical Engineering/Strojniški Vestnik*, 64(11).
- [9] Dudnik, EV, Lakiza, SN, Hrechanyuk, IN, Ruban, AK, Redko, VP, Marek, IO, ... & Hrechanyuk, NI (2020). Thermal barrier coatings based on ZrO<sub>2</sub> solid solutions. *Powder Metallurgy and Metal Ceramics*, 59, 179-200.
- [10] Faktorova, D., Novy, F., Fintova, S., Savin, A., Steigmann, R., Iftimie, N., Turchenko, V. and Craus, M.L., 2016. Evaluation of zirconia coatings deposited on stainless steel substrate. In *Electromagnetic Nondestructive Evaluation (XIX)* (pp. 254-262). IOS Press.
- [11] Wang, Y., Bai, Y., Liu, GH, Sun, J., Zheng, QS, Yu, FL, ... & Wang, HD (2024). Wide-velocity range high-energy plasma sprayed yttria-stabilized zirconia thermal barrier coating—Part II: Structural defects and thermal-bonding properties. *Surface and Coatings Technology*, 476, 130203.
- [12] Qadir, D., Sharif, R., Nasir, R., Awad, A., & Mannan, HA (2024). A review on coatings through thermal spraying. *Chemical Papers*, 78(1), 71-91.
- [13] Asakura, T. and Akamatsu, I., 1972. Fresnel diffraction by a circular aperture illuminated with partially coherent light. I. *Optica Acta: International Journal of Optics*, 19(9), pp.749-763.